

A Point Cloud Completion Approach for the Grasping of Partially Occluded Objects and Its Applications in Robotic Strawberry Harvesting

Ali Abouzeid¹, Malak Mansour¹, Chengsong Hu¹, Dezhen Song¹

Abstract—In robotic fruit picking applications, managing object occlusion in unstructured settings poses a substantial challenge for designing grasping algorithms. Using strawberry harvesting as a case study, we present an end-to-end framework for effective object detection, segmentation, and grasp planning to tackle this issue caused by partially occluded objects. Our strategy begins with point cloud denoising and segmentation to accurately locate fruits. To compensate for incomplete scans due to occlusion, we apply a point cloud completion model to create a dense 3D reconstruction of the strawberries. The target selection focuses on ripe strawberries while categorizing others as obstacles, followed by converting the refined point cloud into an occupancy map for collision-aware motion planning. Our experimental results demonstrate high shape reconstruction accuracy, with the lowest Chamfer Distance compared to state-of-the-art methods with 1.10 mm, and significantly improved grasp success rates of 79.17%, yielding an overall success-to-attempt ratio of 89.58% in real-world strawberry harvesting. Additionally, our method reduces the obstacle hit rate from 43.33% to 13.95%, highlighting its effectiveness in improving both grasp quality and safety compared to prior approaches. This pipeline substantially improves autonomous strawberry harvesting, advancing more efficient and reliable robotic fruit picking systems. Code is available at https://github.com/Malak-Mansour/PointCloud_Completion_for_Grasping

I. INTRODUCTION

Strawberries are a globally popular fruit with significant commercial value, but their cultivation is labor-intensive, particularly during harvesting, which accounts for a substantial portion of production costs [1]. The strawberry industry faces ongoing challenges, including seasonal labor shortages and rising expenses, which have increased interest in automation as a potential solution [2]. The compact size of strawberry plants and the visually distinct appearance of their fruit make them well-suited for robotic harvesting, an area that has attracted growing research interest.

Despite this potential, automating strawberry harvesting presents several challenges, including the fragility of the fruit, which requires gentle, damage-free handling to maintain quality, and the accurate perception of berries in complex, unstructured field environments [3]. Compounding these perception difficulties, robotic systems often struggle to handle partially occluded objects, an issue that remains relatively under-explored in the field [4]. Unlike industrial pick-and-place tasks, where objects are fully visible and structured

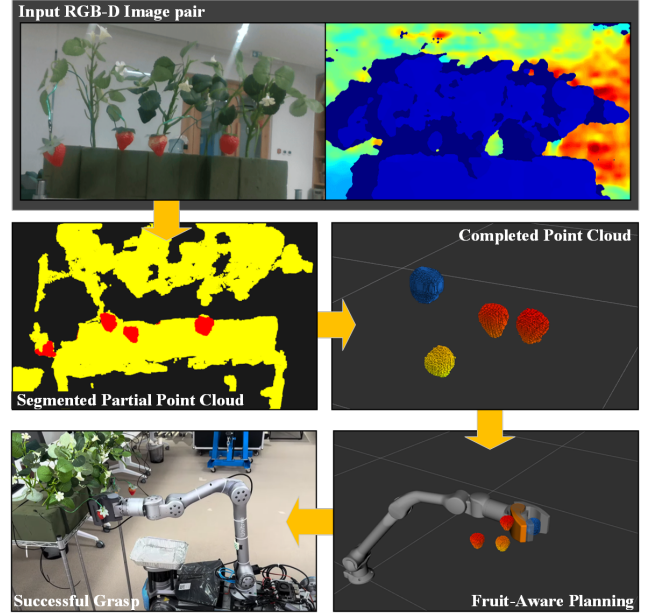


Fig. 1. Top: Input RGB-D image pair showing a multiple strawberry scene. Second row: (left) Segmented point cloud of strawberries, with red points indicating the segmented regions; (right) completed strawberry point cloud after processing the segmented data through a completion model. Bottom row: (right) Planning scene with fruit-aware path planning, where blue points represent the target strawberry and orange/yellow points are treated as obstacles; (left) successful grasping of the target strawberry by the robotic arm using the proposed pipeline

environments aid perception, strawberry harvesting occurs in cluttered settings, where occlusions are common due to leaves, stems, and other fruit, further complicating robotic perception and manipulation.

To enable reliable whole-fruit grasping, a robotic system must acquire detailed semantic and geometric information about target strawberries, even under partial visibility. Here, point cloud completion plays a pivotal role: By reconstructing occluded regions of the fruit, it provides a comprehensive 3D representation of the strawberry, enabling robust grasp planning. This approach not only ensures precise alignment of the gripper to avoid damaging the target fruit through misalignment or excessive force but also identifies and localizes non-target strawberries (e.g., unripe or occluded fruits) that must be avoided during manipulation. By completing partial point clouds of the scene, the system reconstructs both the target's geometry and the surrounding obstacles, bridging the gap between partial sensory input and the complete spatial understanding required for safe, effective autonomous

¹Authors are with the Department of Robotics, Mohamed bin Zayed University of Artificial Intelligence, Masdar City, Abu Dhabi, UAE. Emails:{ali.abouzeid, malak.mansour, chengsong.hu, dezhen.song}@mbzuai.ac.ae

harvesting in real-world conditions. However, a significant hurdle remains: the sim-to-real gap, particularly in handling noisy RGB-D camera data [5], [6]. Existing methods often fail to directly address these discrepancies, limiting their real-world applicability. Fig. 1 demonstrates how our robotic arm successfully grasps the target strawberry without damaging the surrounding strawberries, due to the accurate completion of the partial strawberries' point clouds.

Our main contributions are summarized as follows:

- Robust point cloud processing that reduces sensor noise and bridges the sim-to-real gap through advanced denoising and segmentation.
- Complete 3D reconstruction of occluded or partially visible strawberries, overcoming the limitations of single-view camera captures.
- Accurate grasping of ripe strawberries by treating non-target strawberries as obstacles to avoid damaging them.

Our novel robotic strawberry harvesting pipeline significantly outperforms existing methods in cluttered, real-world environments by addressing these key challenges. Extensive experiments demonstrate significant improvements in grasp success rates and point cloud completion accuracy compared to state-of-the-art methods, as well as a notable reduction in hit rates with non-target strawberries, highlighting the effectiveness of our approach.

II. RELATED WORK

A. Agricultural and Harvesting Robots

Robotic strawberry harvesting has been widely explored to improve labor efficiency and precision. It has been approached primarily through two methods: peduncle cutting [8]–[10] and whole-fruit grasping [11]. While peduncle cutting is a widely adopted method for robotic strawberry harvesting, whole-fruit grasping offers distinct advantages in cluttered environments where occlusions and structural complexity are prevalent. In such settings, leaves, neighboring fruits, and plant structures often obscure the peduncle, demanding highly precise localization and tool maneuverability to execute cuts—a task complicated by limited visibility and spatial constraints [12]. This challenge highlights the need for robust perception and grasp planning strategies. Whole-fruit grasping, in contrast, directly addresses these limitations by leveraging the fruit's larger and more accessible surface area, reducing reliance on pinpoint accuracy.

A key challenge in robotic harvesting is ensuring the visibility of the fruits for accurate detection and manipulation, addressed by leaf manipulation techniques, such as those proposed in [13], [14], which displaces occluding leaves to enhance fruit visibility and improve shape and pose estimation for robotic systems. Furthermore, precise grasp point detection and fruit orientation estimation are essential for effective harvesting, achieved through methods like 3D visual detection that fuse color and geometry to identify graspable regions, such as sweet pepper peduncles for accurate robotic cutting [15]. Grasp point detection can be combined with pose estimation, leveraging either deep

learning-based general feature extraction methods [16], [17] or key points-based estimation methods to recover the main axis of fruits, as demonstrated in [18]–[20].

B. 3D Shape Completion

Shape completion plays a crucial role in reconstructing occluded regions of objects, which is particularly important for applications like robotic harvesting. Various deep learning-based approaches have been developed to address general shape completion tasks. Methods such as DeepSDF [21] and [22] learn continuous shape representations that generalize across both known and unknown shapes, enabling robust shape inference. Extensions like MV-DeepSDF [23] further enhance this by leveraging multi-sweep point clouds for implicit modeling. Attention-based point cloud completion models like PointAttn [7] have been designed to handle general object sets, though they often lack domain-specific adaptations.

In the context of robotic harvesting, shape completion is essential for reconstructing occluded fruit regions to enhance grasping success. While general deep learning methods provide a foundation, they often fail to address the real-time requirements critical for robotic systems. Recent research has addressed these challenges through specialized architectures, particularly the work in [24], which employed transformer networks with contrastive learning and LiDAR priors to enable efficient, real-time completion of occluded fruit shapes.

Building upon these specialized shape completion approaches, a robotic fruit harvesting system was developed based on 3D shape completion with 6-DoF pose estimation for grasping in vertical farms [9]. This system outperforms traditional methods like grasp point detection, orientation estimation, and ellipsoid fitting [15], [16] with higher success rates for strawberries and tomatoes. However, this approach overlooks obstacles around the target fruit, limiting performance in dense clusters. Ellipsoid fitting methods struggle with occlusions due to limited sample points [25], while scene categorization techniques discard occluded fruits entirely [26]. In contrast, our method enables robust fruit harvesting even in cluttered environments by addressing both occlusion and obstacle avoidance.

C. Sim-to-Real Challenges in Robotic Perception

Previous research has tackled the sim-to-real gap in robotic perception using various techniques. R2SGrasp [27] employs a Real-to-Sim Data Repairer (R2SRepairer) to mitigate noise in real depth maps at the data level, enabling real-to-sim adaptation of camera noise. [28] focuses on bridging the simulation-to-real gap for depth images in deep reinforcement learning applications. Other approaches leverage deep learning techniques, such as refinement and self-supervised domain adaptation, to address noise and domain discrepancies [29]. While these deep learning methods are effective, they remain computationally expensive for real-time applications. In contrast, our work tackles the sim-to-real challenge in strawberry harvesting through lightweight

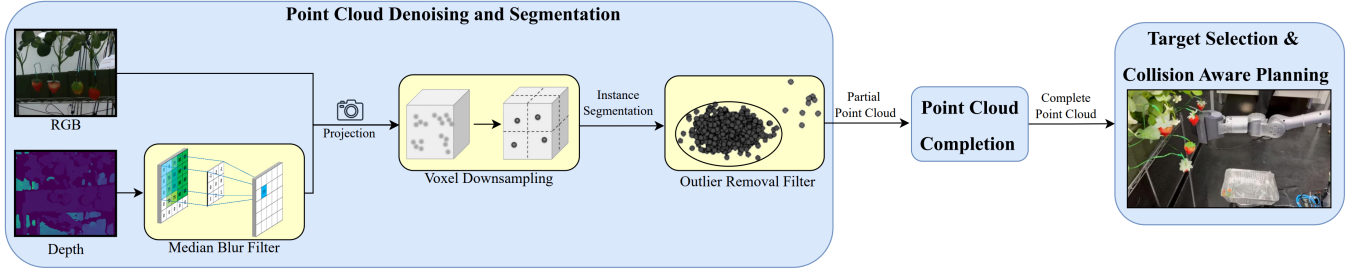


Fig. 2. Our robotic strawberry harvesting pipeline consists of: Point Cloud Denoising and Segmentation, Point Cloud Completion [7], and Target Selection with Collision-Aware Planning, where non-target strawberries are treated as obstacles.

filtering techniques, providing an efficient solution to sensor noise challenges in agricultural robotics.

III. PROBLEM FORMULATION

Given a partially occluded view of the strawberry plant, our method completes the point cloud of the strawberries for accurate grasp planning while treating non-target strawberries as obstacles. Our approach is under the assumption that the strawberry is characterized by a prior fixed shape and size (CAD model) for both training and evaluation.

To formalize our approach, we define key notations and outline the system's input and output representations.

Common notations:

H	Image height
W	Image width
I_{RGB}	RGB image $\in \mathbb{R}^{H \times W \times 3}$
I_D	Depth image $\in \mathbb{R}^{H \times W}$
\mathbf{p}	Input point cloud

Input: The system takes as input an RGB-D image pair, I_{RGB} and I_D , capturing a front-facing view of the strawberry plant.

Output: The system generates a completed 3D point cloud $\mathbf{p}_{i,complete}$ of the i -th strawberry from the partial denoised point cloud $\mathbf{p}_{i,denoised}$. These completed point clouds are then used for obstacle-aware motion planning, where the occupied space is represented as an occupancy map M_{occ} .

IV. ALGORITHM

Our pipeline processes RGB-D images of strawberry plants to enable accurate grasp planning. The approach consists of three main stages: (1) filtering and segmentation to isolate individual fruits, (2) point cloud completion to reconstruct the full 3D shape of each strawberry, and (3) target identification for grasp planning while treating other fruits as obstacles. Fig. 2 illustrates the complete pipeline.

A. Segmenting and Denoising Point Clouds

To generate complete 3D models of individual strawberries from the input RGB-D pair (I_{RGB} and I_D), we implement a multi-stage filtering process that ensures high-quality reconstruction.

We begin with depth image filtering to reduce sensor noise while preserving important edge features. The filtering

operation \mathcal{F} applies a median blur:

$$I_{D,filtered}(u, v) = \text{median} \{ I_D(u', v') \mid (u', v') \in \mathcal{N}_5(u, v) \}, \quad (1)$$

where $\mathcal{N}_5(u, v)$ is the 5×5 neighborhood centered at pixel (u, v) . The filtered depth image is:

$$I_{D,filtered} = \mathcal{F}(I_D). \quad (2)$$

Using $I_{D,filtered}$, we generate a point cloud \mathbf{p} by projecting depth values into 3D space, incorporating RGB information from I_{RGB} and camera intrinsics K :

$$\mathbf{p} = \mathcal{E}(I_{RGB}, I_{D,filtered}, K). \quad (3)$$

To reduce noise further, we apply voxel downsampling \mathcal{V} to \mathbf{p} . Points are grouped into voxels of size $v_s = 0.05$, and their positions are averaged within each voxel. Additionally, we enforce a minimum point threshold per voxel to filter noise:

$$V_i = \left\{ p_j \in \mathbf{p} \mid \left\lfloor \frac{p_j}{v_s} \right\rfloor = i \right\}, \quad (4)$$

where i is the voxel index. The voxel center c_i is computed as:

$$c_i = \frac{1}{|V_i|} \sum_{p_j \in V_i} p_j, \quad \text{if } |V_i| \geq 30, \quad (5)$$

otherwise $c_i = (0, 0, 0)$. The downsampled point cloud $\mathbf{p}_{\text{voxel}}$ is:

$$\mathbf{p}_{\text{voxel}} = \mathcal{V}(\mathbf{p}) = \{c_i \mid i \in \text{voxel indices}\}. \quad (6)$$

Next, we perform instance segmentation on I_{RGB} to generate binary masks $M = \{m_1, m_2, \dots, m_N\}$, where $m_i \in \{0, 1\}^{H \times W}$ corresponds to an individual strawberry, and N is the number of detections. These masks are used to extract points from $\mathbf{p}_{\text{voxel}}$:

$$\mathbf{p}_i = \mathcal{X}(\mathbf{p}_{\text{voxel}}, m_i), \quad (7)$$

where \mathcal{X} isolates points corresponding to mask m_i .

Finally, to enhance the quality of each segmented point cloud, we apply an outlier removal filter \mathcal{O} to eliminate residual noise:

$$\mathbf{p}_{i,denoised} = \mathcal{O}(\mathbf{p}_i). \quad (8)$$

This stage reduces noise, isolates individual strawberries, and ensures high-quality point clouds for further processing.

B. Point Cloud Completion

In line with established approaches for shape completion, we employ a deep learning model based on [7] to learn comprehensive shape representations of strawberries. The model processes a set of denoised partial point clouds and generates their complete counterparts through an encoder-decoder architecture, leveraging pre-trained weights obtained through training on a mix of simulated and real datasets.

The completion network F_θ with parameters θ transforms each denoised point cloud into its complete representation:

$$\mathbf{p}_{i,complete} = F_\theta(\mathbf{p}_{i,denoised}) \quad (9)$$

During training, the model weights θ were optimized using a hierarchical loss function based on Chamfer Distance (CD). The network generates point clouds at different resolutions ($\mathbf{p}_0, \mathbf{p}_1, \mathbf{p}_2$), where \mathbf{p}_0 represents a sparse seed point cloud, and $\mathbf{p}_1, \mathbf{p}_2$ are progressively denser completions. The Chamfer Distance between two point clouds \mathbf{p} and Q is defined as:

$$d_{CD}(\mathbf{p}, Q) = \sum_{p \in \mathbf{p}} \min_{q \in Q} \|p - q\|_2^2 + \sum_{q \in Q} \min_{p \in \mathbf{p}} \|p - q\|_2^2 \quad (10)$$

The total loss is computed against corresponding ground truth point clouds of matching densities:

$$\mathcal{L} = \sum_{i=0}^2 \lambda_i d_{CD}(\mathbf{p}_i, S_i) \quad (11)$$

where λ_i are weighting coefficients and S_i are the ground truth point clouds.

At inference time, we leverage the pre-trained weights for completing the denoised point cloud set. This process generates a set of complete point clouds $\mathbf{p}_{i,complete} \in \mathbb{R}^{n \times 3}$, where n represents the number of points in each completed strawberry point cloud.

C. Target Selection and Motion Planning

Given the set of completed point clouds and their corresponding ripeness labels from the detection stage, we first filter for ripe strawberries to obtain the set of candidate targets $\{\mathbf{p}_{k,complete}\}_{k \in R}$, where R is the index set of ripe strawberries. The optimal target is selected based on minimum Euclidean distance k^* to the end-effector position p_{ee} :

$$k^* = \arg \min_{k \in R} \|c_k - p_{ee}\|_2 \quad (12)$$

where c_k is the centroid of the k -th completed point cloud.

The remaining point clouds, both ripe and unripe, are treated as obstacles:

$$O = \bigcup_{i \neq k^*} \mathbf{p}_{i,complete} \quad (13)$$

These obstacle point clouds are integrated into an occupancy map M_{occ} for collision-aware inverse kinematics:

$$M_{occ} = \mathcal{M}(O) \quad (14)$$

where \mathcal{M} converts the point clouds into a 3D occupancy grid. This allows for motion planning that avoids collisions with other strawberries while approaching the selected target.

Our pipeline is summarized more formally in Algorithm 1.

Algorithm 1 Strawberry Grasping Algorithm

```

1: Input: ( $I_{RGB}, I_D$ ),  $p_{ee}$ 
2:  $\{m_i\}_{i=1}^n \leftarrow \text{DetectRipeNonRipe}(I_{RGB})$ 
3:  $\mathbf{p} \leftarrow \text{GeneratePointCloud}(I_{RGB}, I_D, K)$ 
4:  $\{\mathbf{p}_{i,denoised}\}_{i=1}^n \leftarrow \text{DenoiseAndExtract}(\mathbf{p}, \{m_i\}_{i=1}^n)$ 
5:  $\{\mathbf{p}_k\}_{k \in R} \leftarrow \text{FilterRipe}(\{\mathbf{p}_{i,denoised}\}_{i=1}^n)$ 
6:  $k^* \leftarrow \text{SelectTarget}(\{\mathbf{p}_k\}_{k \in R}, p_{ee})$ 
7:  $\{\mathbf{p}_o\} \leftarrow \{\mathbf{p}_{i,denoised} \mid i \neq k^*\}$ 
8:  $O \leftarrow \emptyset$ 
9: for each  $\mathbf{p}_{i,denoised}$  do
10:    $\mathbf{p}_{i,complete} \leftarrow \text{CompletePointCloud}(\mathbf{p}_{i,denoised})$ 
11:   if  $\mathbf{p}_{i,denoised} \in \{\mathbf{p}_o\}$  then
12:      $O \leftarrow O \cup \mathbf{p}_{i,complete}$ 
13:   end if
14: end for
15:  $M_{occ} \leftarrow \text{GenerateOccupancyMap}(O)$ 
16:  $G \leftarrow \text{EstimateGrasp}(\mathbf{p}_{k^*,complete})$ 
17:  $T \leftarrow \text{PlanTrajectory}(G, M_{occ})$ 
18: if  $T$  is feasible then
19:    $\text{ExecuteGrasp}(T)$ 
20:   return Success
21: end if
22: return Failure

```

V. EXPERIMENTAL SETUP

A. Data Collection

We used a mixture of simulation and real-world data to train our completion model. For simulation data, we utilized NVIDIA Isaac Sim to create a virtual strawberry field with realistic occlusions. We simulated an Intel RealSense D435i RGB-D camera from the robot's perspective to capture partial point clouds of strawberries. This setup allowed us to simultaneously obtain ground truth completed point clouds for training and evaluation.

For real-world data collection, we captured RGB-D data using an Intel RealSense D435i camera in our lab environment, designed to replicate an indoor greenhouse strawberry plantation. The lab setup includes five hanging strawberries with varied arrangements to simulate realistic harvesting conditions. The collected RGB-D data were processed to generate partial point clouds, which were manually annotated for ground truth labeling and combined with the simulation dataset to enhance model robustness. Both the simulation and real-world environments, including the camera perspectives and strawberry field layouts, are shown in Fig. 3.

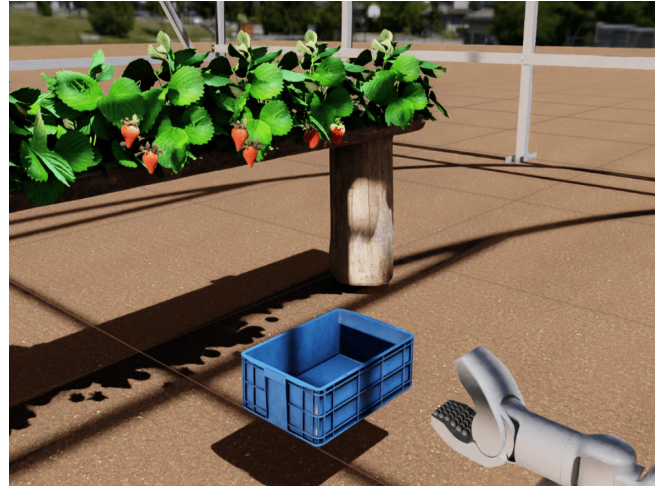


Fig. 3. Simulation and real-world environments for data collection. (Left) Real-world lab setup replicating an indoor greenhouse strawberry plantation. (Right) Simulated strawberry field in NVIDIA Isaac Sim

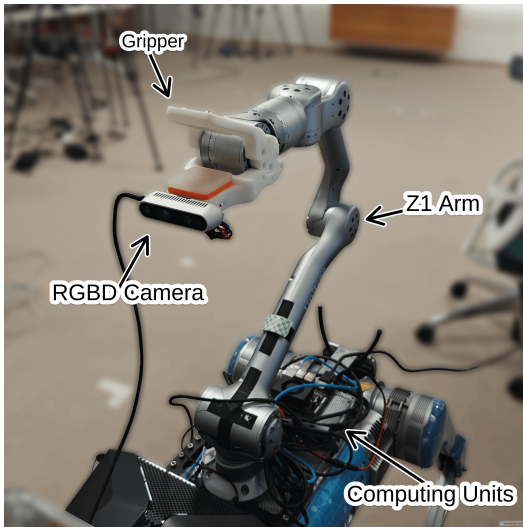


Fig. 4. Robotic system for strawberry harvesting. The image shows the Unitree Z1 robotic arm, grasping mechanism, Intel RealSense D435i RGB-D camera, and NVIDIA Jetson AGX Orin, with annotated components.

B. Robotic System

Once validated in simulation, we deployed our approach on a real-world robotic system designed to replicate an indoor greenhouse strawberry plantation. Our robotic platform consists of a Unitree Z1 robotic arm equipped with a gripper and an Intel RealSense D435i RGB-D camera. The camera is mounted on the robot to capture depth images of five hanging strawberries in a controlled environment. The robot’s computational resources are powered by an NVIDIA Jetson AGX Orin. The robotic system is shown in Fig. 4.

C. Vision Modules

To support our point cloud completion pipeline, we developed vision modules for strawberry detection and segmentation. First, we trained a YOLOv8 [30] model for strawberry detection using RGB images collected from both

the simulation and real-world environments. The training dataset was augmented with variations in lighting, occlusion, and strawberry orientations to improve generalization.

For segmentation, we utilized the Segment Anything Model 2 (SAM2) [31] to generate precise masks for the detected strawberries. The masks were used to refine the partial point clouds, isolating strawberry-specific data for input into our point cloud completion model.

D. Metrics

To evaluate our system’s performance, we conducted 80 real-world trials, using the completed point clouds for obstacle-aware motion planning. We employed several key metrics to assess performance: Attempts Ratio (ρ_a), which measures the ratio of grasp attempts to the number of detections; Success Rate (ρ_s), which calculates the ratio of successful grasps to detections; Success-to-Attempts Ratio (ρ_s/ρ_a), which indicates efficiency by showing how many attempts lead to successful grasps; Chamfer Distance (CD), used as a loss function to measure geometric accuracy of reconstructed point clouds against ground truth data; and Hit Rate (ρ_h), representing the ratio of incidents where other fruits in the scene were hit to the total number of grasp attempts.

E. Baselines

We compare our approach’s success rate to the work in [9], which shares some similarities with our overall approach. Both use point cloud processing, but our objectives differ: our approach specifically aims to grasp strawberries without damaging surrounding fruits in cluttered environments, whereas theirs focuses on individual strawberry grasping. Their setup is based on a vertical farming system and ours on a horizontal one, though the mathematical formulation of the point cloud completion remains similar. Both approaches take a partial point cloud as input and generate a completed point cloud as output, but our method uniquely accounts for

TABLE I
GRASPING SUCCESS RATE RESULTS ON STRAWBERRIES.

Approach	Strawberry		
	$\rho_a \uparrow [\%]$	$\rho_s \uparrow [\%]$	$\rho_s/\rho_a \uparrow [\%]$
Shape Completion [9]	84.38	62.50	74.07
Ours	88.37	79.17	89.58

TABLE II
CHAMFER DISTANCE (CD) RESULTS ON STRAWBERRIES

Approach	$D_C[mm] \downarrow$ avg
CoRe [24]	2.67
DeepSDF-based [32]	2.42
Ours	1.10

neighboring strawberries to enable precise grasping in dense settings.

For chamfer distance evaluation, we compare against [32], which utilizes a pre-trained DeepSDF model to encode the strawberry’s shape representation and employs an occlusion-aware differentiable rendering pipeline for shape completion and pose estimation, as well as [24], which also focuses on reconstructing strawberries in a controlled environment using alternative methods. These approaches provide valuable benchmarks for assessing the accuracy and robustness of our reconstruction framework.

VI. RESULTS AND DISCUSSIONS

Our proposed pipeline effectively integrates point cloud completion with obstacle-aware trajectory planning, surpassing existing methods in both accuracy and robustness in strawberry harvesting.

Grasping Success Rate: As shown in Table I, our method achieves the highest grasping success rate, with $\rho_s = 79.17\%$ and a precision ratio $\rho_s/\rho_a = 89.58\%$, outperforming all baselines. The Shape Completion method [9], the closest competitor, achieves $\rho_s = 62.50\%$, highlighting a relative improvement of 26.67%. This increase is attributed to our accurate pose estimation and obstacle-aware trajectory planning, which enables the robotic arm to execute more stable and precise grasps.

Shape reconstruction accuracy: Table II presents the Chamfer Distance (CD) results, where our method, using PointAttn for point cloud completion, achieves the lowest CD of 1.1 mm, substantially outperforming the best baseline (DeepSDF-based [32]) at 2.42 mm. This indicates that our approach generates more precise 3D shape reconstructions, which is crucial for reliable grasp planning. The improved shape completion ensures better localization of the strawberry’s center and orientation, reducing grasping errors caused by incomplete or noisy point clouds.

Obstacle Avoidance and Grasp Quality: A key advantage of our method is its ability to avoid non-target strawberries, as demonstrated in Table III. When our method is enabled, the obstacle hit rate ρ_h drops dramatically from 43.33% to 13.95%, representing a 67.8% reduction. This indicates that

TABLE III
GRASPING SUCCESS RATE AND OBSTACLE HIT RATE RESULTS ON STRAWBERRIES.

Ours Used	$\rho_s/\rho_a \uparrow$	Obstacle Hit Rate $\rho_h \downarrow [\%]$
×	72.32	43.33
✓	89.58	13.95

our approach significantly improves safety and efficiency in real-world scenarios by minimizing damage to surrounding fruits while maximizing successful harvests.

VII. CONCLUSIONS AND FUTURE WORK

In this paper, we presented a novel robotic strawberry harvesting pipeline that effectively addresses the complex challenges of operating in cluttered agricultural environments by integrating robust point cloud processing with complete 3D reconstruction and obstacle-aware trajectory planning to achieve significant performance improvements in real-world scenarios. The core of our method lies in three technical innovations: our denoising and segmentation techniques that reduce sensor noise and bridge the sim-to-real gap, our point cloud completion model that reconstructs strawberries from single-view RGB-D inputs, and finally a planning framework which treats non-target strawberries as obstacles. Experimental results validate the effectiveness of our approach, demonstrating substantial improvements over existing methods across all performance metrics, with markedly higher grasping success rates while maintaining excellent precision, superior shape reconstruction accuracy with significantly lower Chamfer Distance enabling more reliable grasp planning, and dramatically reduced contact with non-target strawberries, greatly enhancing harvesting safety and efficiency. Despite these promising results, several challenges remain for future work, including incorporating temporal information through multiple viewpoints or active vision strategies, exploring adaptive shape completion methods that can handle greater variability in strawberry sizes, and investigating the integration of this pipeline with different end-effector designs and applications to other high-value crops with similar harvesting challenges. The techniques developed in this work have broader implications beyond strawberry harvesting, potentially benefiting various agricultural robotics applications where precise manipulation in cluttered environments is required, representing a significant step toward more efficient, damage-free automated harvesting systems for delicate crops.

REFERENCES

- [1] J. Guo, Z. Yang, M. Karkee, Q. Jiang, X. Feng, and Y. He, “Technology progress in mechanical harvest of fresh market strawberries,” *Computers and Electronics in Agriculture*, vol. 226, p. 109468, 2024.
- [2] M. Ryan, “Labour and skills shortages in the agro-food sector,” *OECD Food, Agriculture and Fisheries Papers*, no. 189, 2023.
- [3] C. Wang, W. Pan, T. Zou, C. Li, Q. Han, H. Wang, J. Yang, and X. Zou, “A review of perception technologies for berry fruit-picking robots: Advantages, disadvantages, challenges, and prospects,” *Agriculture*, vol. 14, no. 8, p. 1346, 2024.

- [4] H. Zhou, X. Wang, W. Au, H. Kang, and C. Chen, "Intelligent robots for fruit harvesting: Recent developments and future challenges," *Precision Agriculture*, vol. 23, no. 5, pp. 1856–1907, 2022.
- [5] H. Ma, R. Qin, M. Shi, B. Gao, and D. Huang, "Sim-to-real grasp detection with global-to-local rgb-d adaptation," in *2024 IEEE International Conference on Robotics and Automation (ICRA)*. IEEE, 2024, pp. 13 910–13 917.
- [6] J.-B. Weibel, T. Patten, and M. Vincze, "Addressing the sim2real gap in robotic 3-d object classification," *IEEE Robotics and Automation Letters*, vol. 5, no. 2, pp. 407–413, 2019.
- [7] J. Wang, Y. Cui, D. Guo, J. Li, Q. Liu, and C. Shen, "Pointattn: You only need attention for point cloud completion," 2022. [Online]. Available: <https://arxiv.org/abs/2203.08485>
- [8] S. Parsa, S. Parsons, A. Ghalamzan *et al.*, "Peduncle gripping and cutting force for strawberry harvesting robotic end-effector design," in *2022 4th International Conference on Control and Robotics (ICCR)*. IEEE, 2022, pp. 59–64.
- [9] F. Magistri, Y. Pan, J. Bartels, J. Behley, C. Stachniss, and C. Lehnert, "Improving robotic fruit harvesting within cluttered environments through 3d shape completion," *IEEE Robotics and Automation Letters*, 2024.
- [10] S. Parsa, B. Debnath, M. A. Khan, and A. G. E., "Modular autonomous strawberry picking robotic system," *Journal of Field Robotics*, vol. 41, no. 7, pp. 2226–2246, 2024.
- [11] N. K. Uppalapati, B. Walt, A. J. Havens, A. Mahdian, G. Chowdhary, and G. Krishnan, "A berry picking robot with a hybrid soft-rigid arm: Design and task space control," in *Robotics: Science and Systems*, 2020, p. 95.
- [12] B. Zhang, Y. Xie, J. Zhou, K. Wang, and Z. Zhang, "State-of-the-art robotic grippers, grasping and control strategies, as well as their applications in agricultural robots: A review," *Computers and Electronics in Agriculture*, vol. 177, p. 105694, 2020.
- [13] S. Yao, S. Pan, M. Bennewitz, and K. Hauser, "Safe leaf manipulation for accurate shape and pose estimation of occluded fruits," *arXiv preprint arXiv:2409.17389*, 2024.
- [14] E. Gursoy, D. Kulić, and A. Cherubini, "Occlusion handling by pushing for enhanced fruit detection," in *2024 IEEE/RSJ International Conference on Intelligent Robots and Systems (IROS)*. IEEE, 2024, pp. 76–81.
- [15] I. Sa, C. Lehnert, A. English, C. McCool, F. Dayoub, B. Upcroft, and T. Perez, "Peduncle detection of sweet pepper for autonomous crop harvesting—combined color and 3-d information," *IEEE Robotics and Automation Letters*, vol. 2, no. 2, pp. 765–772, 2017.
- [16] N. Wagner, R. Kirk, M. Hanheide, and G. Cielniak, "Efficient and robust orientation estimation of strawberries for fruit picking applications," in *2021 IEEE International Conference on Robotics and Automation (ICRA)*, 2021, pp. 13 857–13 863.
- [17] L. Li and H. Kasaei, "Single-shot 6dof pose and 3d size estimation for robotic strawberry harvesting," 2024. [Online]. Available: <https://arxiv.org/abs/2410.03031>
- [18] J. Le Louëdec and G. Cielniak, "Key point-based orientation estimation of strawberries for robotic fruit picking," in *International Conference on Computer Vision Systems*. Springer, 2023, pp. 148–158.
- [19] C. Zheng, P. Chen, J. Pang, X. Yang, C. Chen, S. Tu, and Y. Xue, "A mango picking vision algorithm on instance segmentation and key point detection from rgb images in an open orchard," *Biosystems engineering*, vol. 206, pp. 32–54, 2021.
- [20] A. Tafuro, A. Adewumi, S. Parsa, G. E. Amir, and B. Debnath, "Strawberry picking point localization ripeness and weight estimation," in *2022 International conference on robotics and automation (ICRA)*. Ieee, 2022, pp. 2295–2302.
- [21] J. J. Park, P. Florence, J. Straub, R. Newcombe, and S. Lovegrove, "DeepSDF: Learning continuous signed distance functions for shape representation," in *Proceedings of the IEEE/CVF conference on computer vision and pattern recognition*, 2019, pp. 165–174.
- [22] Y. Cai, K.-Y. Lin, C. Zhang, Q. Wang, X. Wang, and H. Li, "Learning a structured latent space for unsupervised point cloud completion," in *Proceedings of the IEEE/CVF conference on computer vision and pattern recognition*, 2022, pp. 5543–5553.
- [23] Y. Liu, K. Zhu, G. Wu, Y. Ren, B. Liu, Y. Liu, and J. Shan, "Mv-deepsdf: Implicit modeling with multi-sweep point clouds for 3d vehicle reconstruction in autonomous driving," in *Proceedings of the IEEE/CVF International Conference on Computer Vision*, 2023, pp. 8306–8316.
- [24] F. Magistri, E. Marks, S. Nagulavancha, I. Vizzo, T. Læbe, J. Behley, M. Halstead, C. McCool, and C. Stachniss, "Contrastive 3d shape completion and reconstruction for agricultural robots using rgb-d frames," *IEEE Robotics and Automation Letters*, vol. 7, no. 4, pp. 10 120–10 127, 2022.
- [25] C. F. Lehnert, I. Sa, C. McCool, B. Upcroft, and T. Perez, "Sweet pepper pose detection and grasping for automated crop harvesting," *2016 IEEE International Conference on Robotics and Automation (ICRA)*, pp. 2428–2434, 2016. [Online]. Available: <https://api.semanticscholar.org/CorpusID:47501>
- [26] G. Ren, T. Wu, T. Lin, L. Yang, G. Chowdhary, K. Ting, and Y. Ying, "Mobile robotics platform for strawberry sensing and harvesting within precision indoor farming systems," *J. Field Robotics*, vol. 41, pp. 2047–2065, 2023. [Online]. Available: <https://api.semanticscholar.org/CorpusID:258941446>
- [27] J.-F. Cai, Z. Chen, X.-M. Wu, J.-J. Jiang, Y.-L. Wei, and W.-S. Zheng, "Real-to-sim grasp: Rethinking the gap between simulation and real world in grasp detection," *arXiv preprint arXiv:2410.06521*, 2024.
- [28] Y. Jang, J. Baek, S. Jeon, and S. Han, "Bridging the simulation-to-real gap of depth images for deep reinforcement learning," *Expert Systems with Applications*, vol. 253, p. 124310, 2024.
- [29] X. Siyao, H. Libing, and Z. Shunsheng, "Linear attention based deep nonlocal means filtering for multiplicative noise removal," 2024. [Online]. Available: <https://arxiv.org/abs/2407.05087>
- [30] G. Jocher, A. Chaurasia, and J. Qiu, "Ultralytics yolov8," 2023. [Online]. Available: <https://github.com/ultralytics/ultralytics>
- [31] N. Ravi, V. Gabeur, Y.-T. Hu, R. Hu, C. Ryali, T. Ma, H. Khedr, R. Rädle, C. Rolland, L. Gustafson, E. Mintun, J. Pan, K. V. Alwala, N. Carion, C.-Y. Wu, R. Girshick, P. Dollár, and C. Feichtenhofer, "Sam 2: Segment anything in images and videos," 2024. [Online]. Available: <https://arxiv.org/abs/2408.00714>
- [32] Y. Pan, F. Magistri, T. Læbe, E. Marks, C. Smitt, C. McCool, J. Behley, and C. Stachniss, "Panoptic mapping with fruit completion and pose estimation for horticultural robots," in *2023 IEEE/RSJ International Conference on Intelligent Robots and Systems (IROS)*. IEEE, 2023, pp. 4226–4233.